Limnol. Oceanogr., 47(4), 2002, 1056–1070

Organic matter flux and reactivity on a South Carolina sandflat: The impacts of porewater advection and macrobiological structures

Anthony F. D'Andrea,[1] *Robert C. Aller, and Glenn R. Lopez*
Marine Sciences Research Center, State University of New York at Stony Brook, Stony Brook, New York 11794-5000

Abstract

Study of the flux and fate of reactive organic material (OM) within Debidue Flat, an intertidal sandflat in the North Inlet estuary, South Carolina, demonstrated that this coarse-grained deposit is a dynamic, open system that experiences rapid OM decomposition and exchange of solutes in the top 30 cm of the sediment column. The fluxes of reactive OM through Debidue Flat were high during all seasons (27–170 mmol C m^2 d^{-1}) and were comparable to fluxes in muddy portions of the North Inlet estuary. Porewater decomposition products were N- and P-rich, the modeled reactivity of organic carbon undergoing decomposition was high (first-order rate constant, $k = 0.02$ d^{-1}), and abundant extractable chlorophyll *a* was measured year-round; all properties were consistent with marine algal-derived substrates. Porewater solute profiles were controlled by advective flow that rapidly exchanged porewater with overlying waters to ~25 cm depth on timescales of hours. Thus, these sandflats act like an unsteady ''trickling bed filter,'' capturing or generating reactive organic particles, rapidly remineralizing OM, and recycling nutrients. Macrobiological structures within the flat altered the amounts and reaction rates of OM on various spatial and temporal scales. Relatively elevated OM decay rates were associated with the burrows of *Callichirus major,* a deep-burrowing thalassinid shrimp. Large stingray feeding pits accumulated fine grained OM, locally clogging the ''trickling bed filter,'' and inhibiting porewater advection. As illustrated by Debidue Flat, intertidal sands can be sites of high OM flux and turnover and play an important role in biogeochemical cycling in estuarine systems.

Much of the work on benthic biogeochemical cycling has centered on organic-rich muds. Organic matter remineralization in low carbon sands, however, can have rates comparable to those in organic rich muds (Rowe et al. 1988, Cammen 1991; Grant et al. 1991). Porewater advection results in the rapid exchange of pore and overlying water and has been implicated as the primary process responsible for enhancing remineralization rates and carbon cycling in sands.

Physical and biological structures, tidal currents, and waves create pressure gradients that can drive advective porewater flow deep into permeable sandy sediments (Shum and Sundby 1996; Huettel and Webster 2001). These flows move along two- or three-dimensional flowpaths and can increase the effective diffusion coefficients of permeable sediments 5–10 times (Vanderborght et al. 1977; Huettel and Gust 1992). Intertidal systems can also have gravitational (e.g., McLachlan 1989) and convective exchange (e.g., Rocha 1998, 2000) of pore and overlying waters during tidal exposure and subsequent flooding. Advective porewater flow is an effective mechanism for rapid exchange of oxygen (Forster et al. 1996; Ziebis et al. 1996*a*), dissolved and particulate organic matter (OM; Huettel et al. 1996; Huettel and Rusch 2000), and nutrients (McLachlan et al. 1985; Huettel et al. 1998; Rocha 1998) in permeable sediments.

Recent work by Ziebis et al. (1996*a*,*b*) and Huettel et al. (1996, 1998) has demonstrated that the presence of active macrobiological structures, in particular crustacean burrows and mounds, also has a significant impact on porewater solute gradients and fluxes across the sediment-water interface of coarse-grained deposits. Macrobiological activities can also strongly influence transport-reaction processes in shallow coastal systems by effectively increasing the oxygenated surface area of the sediment-water interface, enhancing coupling between redox reactions, stimulating microbial growth rates, and promoting rapid exchange of porewater and overlying water solutes across the sediment-water interface (Aller 1988, 2001; Kristensen 1988). Along the coast of South Carolina, burrowing and feeding by the thalassinid shrimp *Callichirus major* and the formation of stingray feeding pits increase the flux of nutrients and organic matter on zonally dependent spatial scales and alter sediment permeability by the introduction of fine particles.

Although there have been a number of sophisticated modeling and flume studies of transport and biogeochemical processes in permeable sediments, field studies of carbon cycling in estuarine sand bodies remain few. In this work, we document the dynamics of reactive organic matter remineralization processes on Debidue Flat, an intertidal sandflat in the North Inlet estuary, S.C. OM remineralization rates, N/P stoichiometries of decomposition, and OM reactivity were quantified seasonally using a combination of anoxic incu-

[1] Corresponding author (dandrea.tony@epa.gov). Present address: US EPA, Pacific Coastal Ecology Branch, 2111 SE Marine Science Drive, Newport, Oregon 97365.

Acknowledgments

We thank Joe D'Andrea, Bonnie Willis, Karen Hudson, and Ryan Pigg for their help during field work. We would also like to acknowledge the Belle W. Baruch Marine Laboratory for providing laboratory and office space and Bill Johnson for the use of the chemical laboratory. We appreciate the comments and discussions of S. A. Woodin, R. M. Cerrato, D. Conley, and H. A. Stecher. This study was supported by a graduate research fellowship awarded to A.F.D. by the National Oceanic and Atmospheric Association National Estuarine Research Reserve Program. Additional funding was provided by research grants to G.R.L. from the National Science Foundation (OCE9711793) and Office of Naval Research (N00014931604). R.C.A. was supported by NSF grant OCE9730933. This paper is contribution 1238 of the Marine Sciences Research Center and contribution 1343 of the Belle W. Baruch Institute for Marine Biology and Coastal Research.

Table 1. Summary of sampled environments, time points, and depth intervals sampled for the three seasonal whole-core incubations.

Incubation	Sampled environments	Time points (days)	Depth intervals (cm)
Fall 1997	SF, CM, RP	0, 7, 14, 21	0–5, 5–10, 10–15, 15–20, 20–30
Winter 1998	SF, CM	0, 7, 14, 21	0–5, 5–10, 10–15, 15–20, 20–30, 30–40
Summer 1998	SF, CM	0, 3, 7, 14, 21, 35, 62, 135	0–5, 5–10, 10–15, 15–20, 20–30, 30–40

CM, *C. major* burrows; RP, ray pits; SF, sandflat.

bations and chlorophyll *a* profiles. Experiments were also designed to distinguish reaction rates and fluxes between the general sandflat surface and regions locally affected by burrows of the common thalassinid shrimp, *C. major*. In addition, field experiments were conducted to quantify in situ hourly changes in reactive porewater constituents as tidal flow varied from before slack low tide to subsequent flood. This series of observations allowed the documentation of porewater profiles in the vicinity of *C. major* burrows, ray pits, and the sandflat and distinguished the effect of the dominant passive advection due to tidally driven currents from active, macrofauna-driven advection on Debidue Flat.

Methods

Study site—Debidue Flat is located within the North Inlet estuary near Georgetown, South Carolina (33°19′N, 79°08′W). This intertidal sand flat is within 0.5 km of the inlet and is a remnant flood tidal delta associated with the position of the mouth of North Inlet in 1878. Debidue Flat has been a stable feature for >30 yr with annual periods of erosion in early fall, deposition from March through May, and stability during the summer; these patterns are directly associated with depositional and erosional events of the nearby beaches (Humphries 1977). The tidal channel that drains Debidue Flat is dominated by ebb-tidal currents (Kjerve and Proehl 1979), with minimal wave action due to its location behind Debidue Island. Salinities are usually high (29–35), and freshwater runoff is negligible. The sediments on this flat are well-sorted medium-fine sand (2.35 ϕ) and have a fairly uniform porosity (mean, 0.40 ϕ) and low organic content (<0.04% dry wt) (Grant 1981; D'Andrea unpubl. data). The macrosurface topography is dominated by ebb-oriented surface ripples (15–20 cm wavelength, 3–5 cm amplitude), dasyatid ray pits, and *C. major* burrows.

Remineralization rates—Time series, whole-core anoxic incubations (Aller and Mackin 1989) were used to estimate rates of ΣCO_2, DOC, and NH_4^+ production rates in the vicinity of *C. major* burrows and on Debidue Flat in fall (September) 1997, winter (January) 1998, and summer (June) 1998. This type of incubation has been shown to give estimates of carbon remineralization rates consistent with alternative methods (Mackin and Swider 1989).

The cores used in these experiments were 7.65 cm (inside diameter) by either 30 cm (September) or 45 cm (January and June) in length. Holes drilled on opposite sides along the length of core tubes at 1-cm intervals were threaded to accommodate ports for porewater sampling and were sealed with electrical tape to prevent loss of porewater before sampling. Cores for each experiment were collected within 3 d of each other to minimize temporal variability and were collected while the sandflat was submerged, to ensure porewater at all depths. Immediately after collection, both ends were sealed with plastic-wrapped rubber caps and the cores were transported to the laboratory. After 24 h, macrofauna would come to the surface of the core and were removed to reduce any bias in the results from their decay. Each core was sealed after excluding air by adding neoprene spacers that fit inside the core. They were incubated within buckets (fall) or trash cans (winter and summer) filled with mud to ensure anoxic conditions. The buckets or trash cans were nested in storage tanks with ambient flowing seawater to maintain field temperatures during the incubation.

Decomposition rates in the vicinity of *C. major* burrows were distinguished from ambient rates for Debidue Flat by defining the regions within 10 cm of *C. major* burrows as directly impacted (CM). Cores collected ~50 cm away from burrows were assumed to represent reactive carbon decomposition processes typical of the generally rippled sandflat surface (SF). The four–five cores collected per sampled environment and time point within each seasonal incubation were sampled only once. The sampled environments, time points sampled, numbers of cores, and depth intervals collected for the incubations are summarized in Table 1.

Porewaters from three–four cores per treatment were sampled at each time point by pushing screw-in ports through the electrical tape and tightening them until they were flush with the core. Initially 1 ml of porewater collected by syringe was discarded before the sample for each depth interval (3–4 ml) was collected. Samples were taken successively from the top to the bottom of vertically oriented cores to prevent subduction of porewater from intervals above the sampled depth. Sediments were sufficiently permeable to permit direct sampling of porewater with negligible clogging. Preliminary experiments conducted with layered dyes confirmed that the samples collected (4–5 ml) were sufficiently small so that sampling did not cause percolation from portions of the core outside the 5- or 10-cm zone of sampling. Immediately after collection, porewater was filtered (0.4 μm) into acid-washed vials. Porewater was evenly divided between vials for NH_4^+ and dissolved carbon analyses. Samples were stored in coolers until transported to the analytical laboratory. No NH_4^+ samples were taken in the September 1997 incubation.

Samples for NH_4^+ analysis were frozen until analyzed (usually within a week). Samples were defrosted within coolers, diluted as appropriate, and analyzed for dissolved

NH_4^+ by use of a Technicon Autoanalyzer or by manual colorimetric techniques modified from Solorzano (1969). To quantify adsorbed NH_4^+ and the reversible adsorption coefficient for sandflat sediments, individual cores from five time points in June 1998 were sectioned into intervals corresponding to porewater sampling (Table 1). Each sediment sample was homogenized by hand, and ~1–2 g wet weight was placed in preweighed 15-ml centrifuge tubes; 2N KCl was added to the tubes in a ~10 : 1 ratio of KCl (ml) to wet weight sediment (g). Tubes were shaken for ~1 h at ~22°C, centrifuged at 550 × g for 5 min, and the supernatants were filtered (0.4 μm) into acid-washed vials. KCl extractions were analyzed for NH_4^+ on a Technicon Autoanalyzer. Sediment remaining in centrifuge tubes was rinsed two–three times with deionized-distilled water to remove salts and dried for 36 h at 60°C. Exchangeable NH_4^+ concentrations (KCl extraction corrected for porewater contribution) were plotted against the corresponding porewater concentrations, and the dimensionless adsorption coefficient, *K*, was calculated from the slope (Rosenfeld 1979). Net production of porewater NH_4^+ during incubations were converted to gross NH_4^+ production by multiplication of the observed rates by the factor $(1 + K)$. The adsorption coefficient, *K*, for this system was estimated to be 0.65 on the basis of the linear relationship between measured porewater ammonium and exchangeable ammonium in both of the seasons in which ammonium was measured.

Samples for dissolved carbon analysis were typically analyzed immediately or refrigerated until analyzed (within 1–2 d). Porewater samples were analyzed for ΣCO_2 (September) or ΣCO_2 and dissolved organic carbon (DOC) (January and June) by use of a Shimadzu TOC-500 carbon analyzer. Each sample was analyzed in triplicate and rerun if the coefficient of variation between replicates was >5%. Samples analyzed for DOC were initially analyzed for ΣCO_2, then two–three drops of 10% HCl were added, and each was sparged with N_2 to remove inorganic carbon. Samples were then analyzed for DOC.

Reaction rates and fluxes from whole-core incubations—The reaction rates and fluxes in the whole-core experiments were estimated from changes in ΣCO_2, DOC, and NH_4^+ profiles over the course of the experiment by use of two methods: linear regression and an analytical model to correct for diffusion. The change in concentration for a given depth interval over the course of 21 or 35 d was modeled by use of linear regressions. These estimates, however, do not account for internal diffusion in the cores during the experiments. To account for internal diffusion, the changes in solute profiles between sampling times were also modeled by use of an analytical transient-state diffusion-reaction model corrected to the incubation temperature, as described in appendix 1 of Aller et al. (1996). This model corrects for internal diffusion within the whole core incubations over the 21 or 35 d in which reaction rates were estimated. Carbon to nitrogen reaction stoichiometry was quantified by calculating $R_{\Sigma CO_2}/R_{NH_4^+(1+K)}$ for each depth in both the sandflat and *C. major* burrow incubations. Here $R_{NH_4^+(1+K)}$ represents the gross ammonium production rate. The volumeric reaction rates measured in the incubations were used to estimate the areal fluxes of reactive organic carbon (OC) under the assumption of a 1 : 1 molar ratio between OC remineralized and dissolved carbon produced in the porewaters. These values are estimates of in situ carbon fluxes for the system at the time of core collection (Aller and Mackin 1989; Mackin and Swider 1989).

Carbon and nitrogen reactivity, summer 1998—The reactivity of the organic material (OM) undergoing decomposition in the whole-core incubations was investigated by extending incubations over 135 d in the June 1998 incubation to follow the concentration and production rate patterns of ΣCO_2, DOC, and NH_4^+ (see Table 1). Conceptually, the decomposition rate of a single reactive pool within a core can be described by an exponential relationship with the concentration of the products with time and depth governed by changes in the reaction rate:

$$R(z,t) = R_0 e^{-kt} e^{-az} + R_\infty e^{-kt}$$

where $R(z,t)$ is the reaction rate at a given depth and time; (R_0) is the reaction rate at $t = 0$ and $z = 0$, k is the reactivity constant (d^{-1}), t is the time (d), α is the attenuation factor, and z is the depth in the sediment (cm). The average concentration over the entire core (40 cm), C_{avg}, is related to the core-averaged reaction rate, *Ravg*, at a given time:

$$C_{avg}(t^*) = \int_0^{t^*} R_{avg}(t)\, dt + C_o \quad \text{and}$$

$$R_{avg}(t) = \frac{\int_0^{z^*} R(t)\, dz}{z^*}$$

where t^* is the sampling time point, z^* is the sampling depth, and C_o is the original concentration. After substituting our assumed relationship for reaction rate into the above relationship, the expected pattern can be described as

$$C(t) = (C_\infty - C_o)(1 - e^{-kt}) + C_o$$

where C_∞ is the asymptotic concentration. The weighted average concentrations in cores at each of the time points in the June 1998 incubation were modeled based on the expected relationship above to estimate the reactivity constant (k) and the initial and asymptotic dissolved carbon concentrations (total reactive pool size). The two sampled environments (SF and CM) and the different dissolved carbon (ΣCO_2, DOC) components were modeled separately.

Seasonal Chl a *profiles*—Vertical depth profiles of Chl *a* were collected seasonally in conjunction with whole-core incubations, particle-mixing experiments (D'Andrea et al. unpubl. data), and porewater sipper experiments (see below). Replicate cores (2–9) were collected in June and September 1997 and January and June 1998. Cores were extruded in 0.5-cm intervals for the first 1 cm, 1-cm intervals to 5 cm, 2.5-cm intervals to 10 cm, and 10-cm intervals to the base of the core (typically 40 cm). Subsamples of each depth interval were stored in 20-ml scintillation vials at −80°C until analysis. Chl *a* was extracted from ~1g of sediment (wet wt) for 24 h in the dark at 4°C by use of 10 ml of 100% acetone and analyzed by use of a Sequoia-Turner

Model 450–003 fluorometer. Chl *a* concentrations are reported here in units of μg g^{-1} dry weight sediment. Additional deep samples were collected in April 1999 to quantify the depth and concentration of background Chl *a* values for this sandflat. Four cores were collected covering depths from 35 cm to 1 m in ~10-cm depth intervals. Samples were analyzed immediately for Chl *a* as described above.

Porewater sippers—Changes in porewater concentrations were measured by use of multiple porewater sippers (modified after Huettel 1990). The sampler consisted of a hollow 2.5-cm diameter PVC pipe with 6-mm diameter holes drilled on both sides of the pipe at 2-, 5-, 10-, 15-, 20-, and 25-cm depths. Each of these paired holes was fitted with a porous (60 μm) polyethylene diffuser tube (6 mm outer diameter and 3 mm inner diameter; Labpor Porous Products, Porex Technologies, Fairburn, GA). Paired diffuser tubes were connected to 60-ml syringes by Tygon tubing with 1-mm inner diameter. Samples were collected by drawing sequentially deeper samples by use of the syringes. An overlying water sample was collected at the same time as porewater samples, for comparison.

The susceptibility of the porewater sippers to mixing with overlying water was tested in the laboratory by use of a bucket of seawater-saturated sand placed in a 30 gallon trashcan and slowly covering the bucket with ~10 cm of freshwater. The sipper was then pushed into the sand, and three sets of 20-ml samples were collected and analyzed for Cl^- by use of a potentiometric titrator (Radiometer CMT 10 titrator). There was no noticeable difference between the initial chloride profiles and the three collected profiles after the introduction of essentially chloride-free overlying water.

Porewater samples were collected 18–20 August and 1 and 3–5 November 1998. Two sippers were deployed on each day. One sipper was placed either within a ray pit (19 August and 4–5 November) or within 5 cm of a *C. major* burrow (18 and 20 August and 1 and 3 November). The second sipper each day was placed at the same tidal height as the first sipper but was 50 cm away from both ray pits and *C. major* burrows. The second sipper was considered the sandflat treatment in the absence of macrobiological structure effects. Sippers were allowed to equilibrate for at least 1 h before sample collection. Concurrent samples were collected from each depth interval approximately hourly from both sippers starting 2 h before low tide and ending 4 h later.

The first 2 ml was discarded before 20 ml was drawn from each depth interval. A PVC disc placed on the sediment surface prevented sampling overlying water. Ten milliliters of each sample was immediately transferred to a 10-ml syringe for dissolved oxygen analysis (described below). The remaining sample from each syringe was filtered through a 0.4-μm syringe filter into an acid-washed glass vial that was placed on ice in the dark until transported to the laboratory.

Porewater was analyzed for NH_4^+, NO_3-NO_2, and PO_4 within 18 h of collection by use of two separate Technicon autoanalyzers, one for NH_4^+ and a second for both PO_4 and NO_3-NO_2. This permitted rapid nutrient analysis that minimized contamination or storage effects. Samples for dissolved carbon analysis were typically analyzed immediately or refrigerated until analyzed (within 3 d). Samples were analyzed for ΣCO_2 and DOC by use of a Shimadzu TOC-500 carbon analyzer.

Oxygen in porewater samples was determined on unfiltered samples by use of a modified microwinkler technique (Strickland and Parsons 1972). The lower operational limit of this technique was determined by collecting a bucket of sand from Debidue Flat, allowing the sand to go anoxic for ~30 d, and measuring the dissolved oxygen profiles from porewater samples collected by use of the sipper. The lower limit was 20 μM O_2.

The stoichiometries of the net reactions producing or removing the porewater constituents were evaluated. Geometric mean regressions were used to compare ΣCO_2 : total dissolved inorganic nitrogen (DIN), total DIN : PO_4, and O_2 : total DIN stoichiometries. Slopes were used as estimates of C : N, N : P, and O_2 : N reaction ratios.

Results

Reaction rates, stoichiometry, and fluxes—The rates of change of ΣCO_2 and NH_4^+ within individual depth intervals with time were used to estimate reaction rates for the incubations assuming no transport between intervals. The transport-reaction model, which accounted for solute diffusion within the incubated core, was also fitted to entire whole core profiles with time to obtain best fit reaction functions. The two types of estimates are compared for net ΣCO_2 reaction rates in Fig. 1A. The highest reaction rates occurred in the top 5 cm and decreased exponentially with depth. Reaction rates associated with *C. major* burrows in fall 1997 were greater at all depth intervals relative to the sandflat. Reaction rates at the base of these cores were ~60% of the rate estimated in the top 5 cm. Carbon production rates in the winter 1998 incubation followed a similar pattern with ΣCO_2 reaction rates associated with *C. major* burrows always higher than the sandflat cores. This is particularly evident in the deep portion of the cores (20–40 cm), where reaction rates associated with shrimp burrows were ~2 times higher. The ΣCO_2 production rates in summer 1998 were similar between the sandflat and *C. major* burrow environments (Fig. 1A). The estimated and transport modeled reaction rates were slightly higher at all depths in the sandflat treatment, and there was not a noticeable effect of *C. major* burrows on ΣCO_2 production at depth.

Ammonium production rates were measured only in the winter and summer 1998 incubations (Fig. 1B). The pattern observed in winter 1998 NH_4^+ production rates was similar to that observed for ΣCO_2 production, with reaction rates in the deeper portion of *C. major* burrow cores 3–4 times higher than sandflat cores (Fig. 1B). In contrast, NH_4^+ production rates in the June 1998 incubation showed deviations from the patterns in carbon production. This is most noticeable below 15 cm, where *C. major* burrows showed production rates 2–3 times higher than those found in the sandflat treatment. Sandflat cores were characterized by a gradual exponential decrease to low reaction rates at depth. Ammonium production rates in the vicinity of *C. major* burrows had a rapid exponential decrease in the top 10 cm, leveling off to

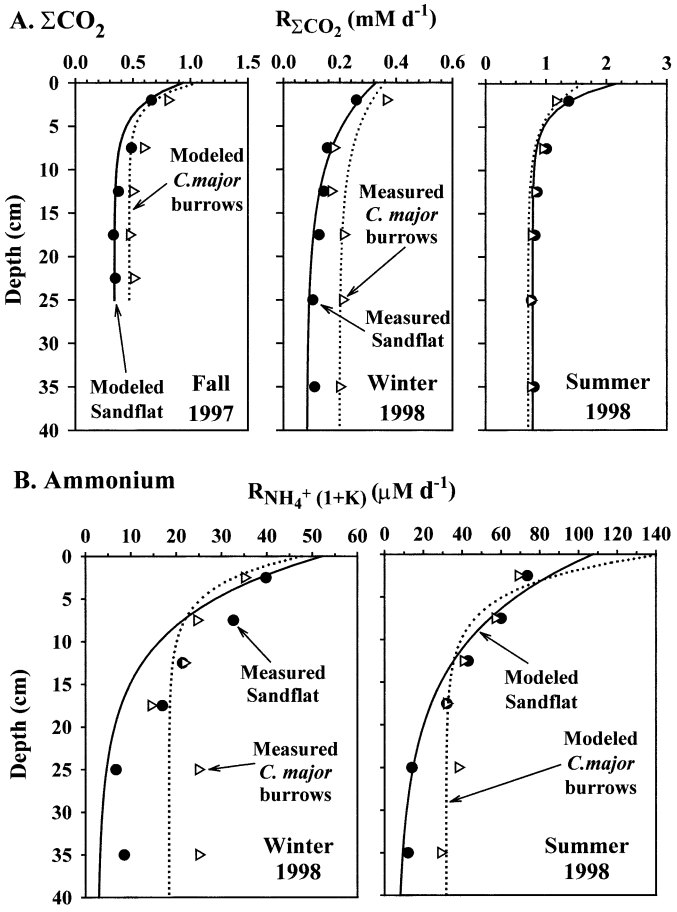

Fig. 1. (A) ΣCO_2 and (B) adsorption-corrected ammonium production rates in seasonal whole-core incubation experiments. Reaction rates are presented as least-squares estimates and modeled diffusion-corrected rates.

a constant value to the base of the core. Modeled reaction rates associated with shrimp burrows were always higher than the sandflat in the deeper portions of the cores (>15 cm).

Carbon to nitrogen production stoichiometry with depth in the cores was determined in winter and summer 1998. The magnitude of the C : N ratio differed between the two time points, but the relative patterns associated with the two sampled environments were consistent and strikingly different. The surface C : N ratio of decomposition was lower in January (~6–8) relative to the June incubations (~10–15). In both incubations, sandflat cores had low C : N ratios in surface sediments with a steady increase with depth in the core (Fig. 2). In contrast, the C : N ratio associated with shrimp burrows showed an initial slight increase with depth followed by a steady ratio beginning at 10–15 cm depth.

Carbon and ammonium fluxes had a strong seasonal component and were impacted by the presence of *C. major* burrows. Estimated reactive carbon fluxes were highest in summer 1998, intermediate in fall 1997, and lowest in winter 1998 (Fig. 3). Carbon fluxes associated with *C. major* burrows in the fall incubation were 30% greater than the sandflat. Carbon fluxes in the winter incubation decreased

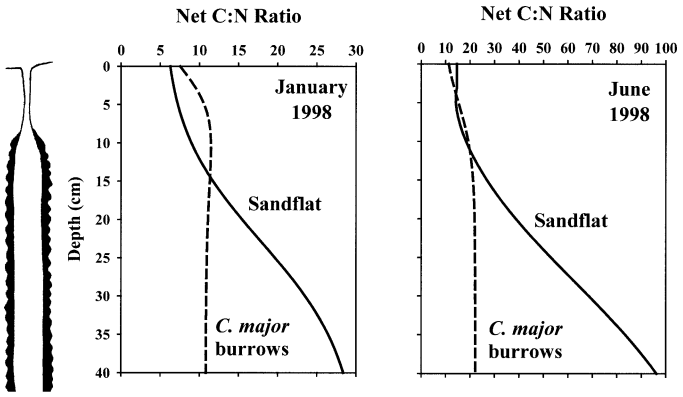

Fig. 2. Net C : N stoichiometry with depth in the winter and summer 1998 whole-core incubation experiments for Debidue Flat and in the vicinity of *C. major* burrows. The general structure and dimensions of the top 40 cm of *C. major* burrows on Debidue Flat are shown next to the figures.

~40%–50% in both the sandflat and *C. major* environments relative to the fall incubation experiments. The carbon fluxes in the vicinity of *C. major* burrows were comparable to the fluxes estimated for the sandflat in the fall incubation. Es-

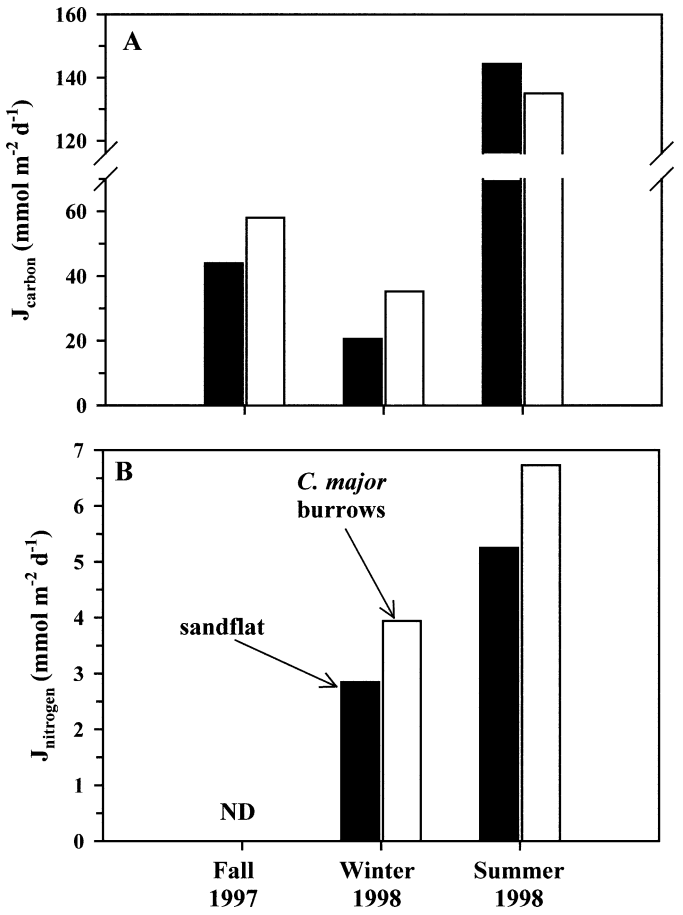

Fig. 3. Estimated fluxes across the sediment-water interface of (A) reactive OC and (B) nitrogen from whole-core anoxic incubations for sandflat and *C. major* burrows.

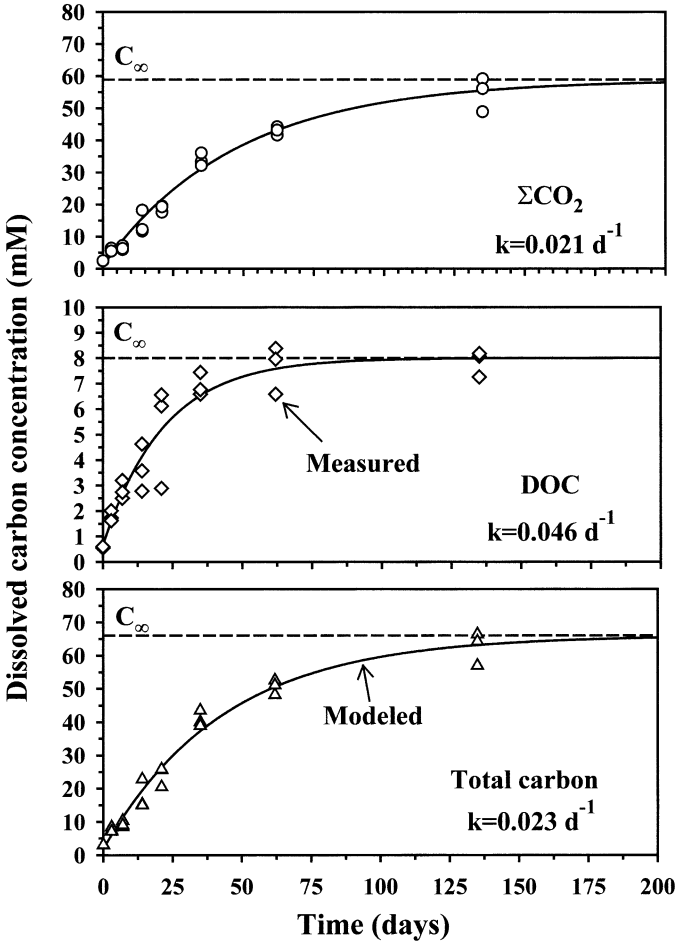

Fig. 4. Comparison among modeled and measured ΣCO_2, DOC, and total carbon concentrations for the sand flat whole-core incubation in summer 1998. The reactivity constant (k) for each component is indicated on the figure. The horizontal dashed lines indicate the predicted asymptotic concentration, C_∞.

timated carbon fluxes were greatest in summer, with values three to four times greater than any other time point. Summer 1998 was also the only incubation with comparable carbon fluxes for both the sandflat and shrimp burrows. The proportion of the reactive carbon production flux attributed to DOC was comparable between sandflat and *C. major* burrows, ranging from ~8% in the winter to ~15% of the total flux in the summer (data not presented). Ammonium fluxes consistently showed an effect of *C. major* burrows, with fluxes 30%–80% greater than the sandflat (Fig. 3). Ammonium flux from the winter to summer incubations approximately doubled.

Carbon reactivity—Figure 4 compares the modeled production of the various carbon components to the depth averaged concentrations from the cores in the whole-core incubations. The exponential model effectively describes the production of carbon in the porewaters with time. There is no apparent difference between the modeled reactivities between the sandflat and shrimp burrows, with a first-order reactivity constant (k) of 0.02 d^{-1} for the OC being decomposed. DOC production is characterized by a distinctly greater reactivity, which suggests release from a particularly labile subpool (cell lysis?); however, overall C production pattern is dominated by ΣCO_2.

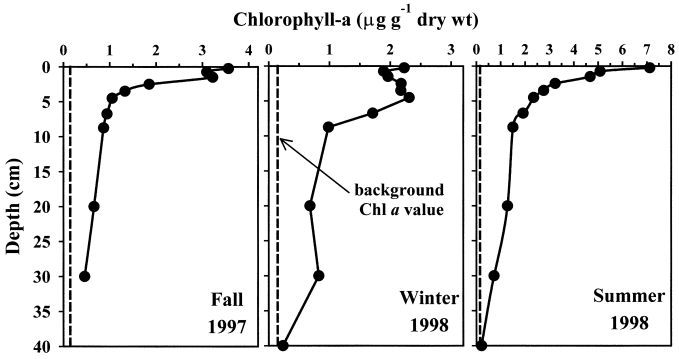

Fig. 5. Vertical Chl *a* depth profiles in fall 1997, winter 1998, and summer 1998. Points are plotted as means. The vertical dashed line represents background Chl *a* value for this system as based on deep Chl *a* samples.

Chl a *profiles*—The surface concentrations (top 1 cm) of Chl *a* on Debidue Flat were high and varied with season, ranging from a low of 2.2 μg g^{-1} in winter 1998 to a high of 7.1 μg g^{-1} in summer 1998 (Fig. 5). Concentrations of Chl *a* on the sandflat generally decreased exponentially with depth. The background concentration of Chl *a*, determined by use of the deep core samples (50–100 cm), was 0.14 μg g^{-1} and never occurred shallower than 45 cm. The depth penetration of Chl *a* also varied with season with shallower penetration in the fall relative to the winter and summer samples.

Porewater sipper experiments—The purpose of the porewater sipper experiments was to tease apart the porewater solute patterns associated with macrobiological structures and the general sandflat surface. Ideally, the deployment of the sippers was at a tidal height, leaving a couple centimeters of overlying seawater above the sediment surface at low tide. This did not always occur, was further complicated by the prevailing winds on the day of sampling, and was particularly evident during sipper deployment in 3–5 November 1998. The remnants of hurricane Mitch maintained steady winds (9–13 knots) and tidal currents over the study area and prevented the isolation of porewater solute profiles in the absence of porewater advection for these dates; those data will not be presented here. This resulted in 3 d of usable data in which the absence of porewater advection was maintained at low tide—18 and 20 August 1998, with sippers deployed at *C. major* burrows and the sandflat and 19 August 1998, with deployment within a ray pit and the sandflat.

Solute profiles near Callichirus major *burrows*—The porewater profiles of inorganic nutrients were impacted by the presence of *C. major* burrows. Profiles of NH_4^+ 1 h before low tide are approximately vertical in both the sandflat and in the vicinity of *C. major* burrow (Fig. 6A). At slack low tide but with water still over their burrows, the actively

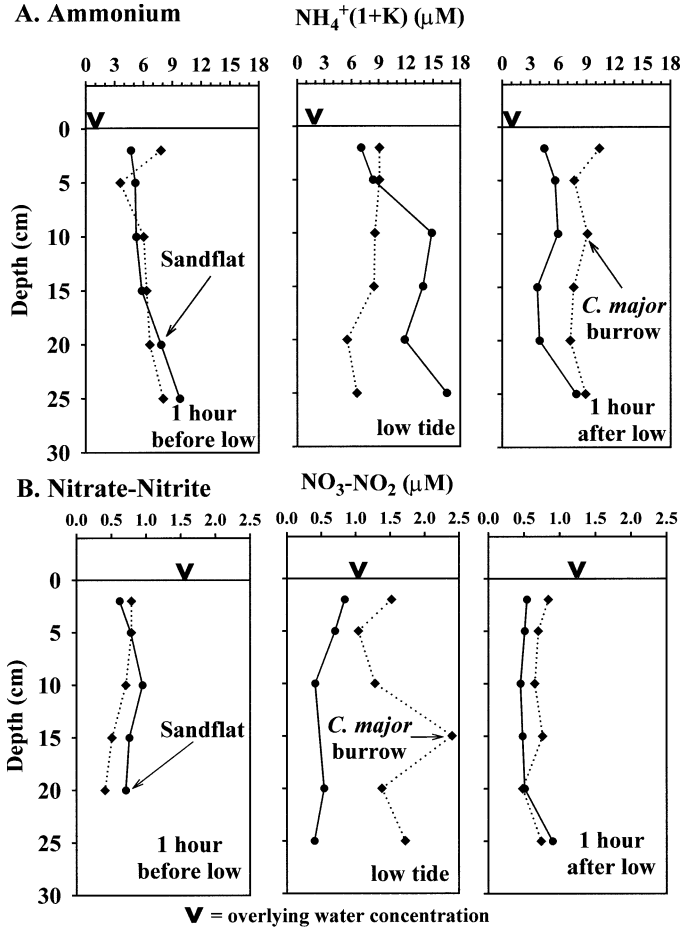

Fig. 6. Porewater profiles of (A) adsorption-corrected ammonium and (B) total NO_3 + NO_2 for the sandflat and an active *C. major* burrow on 20 August 1998.

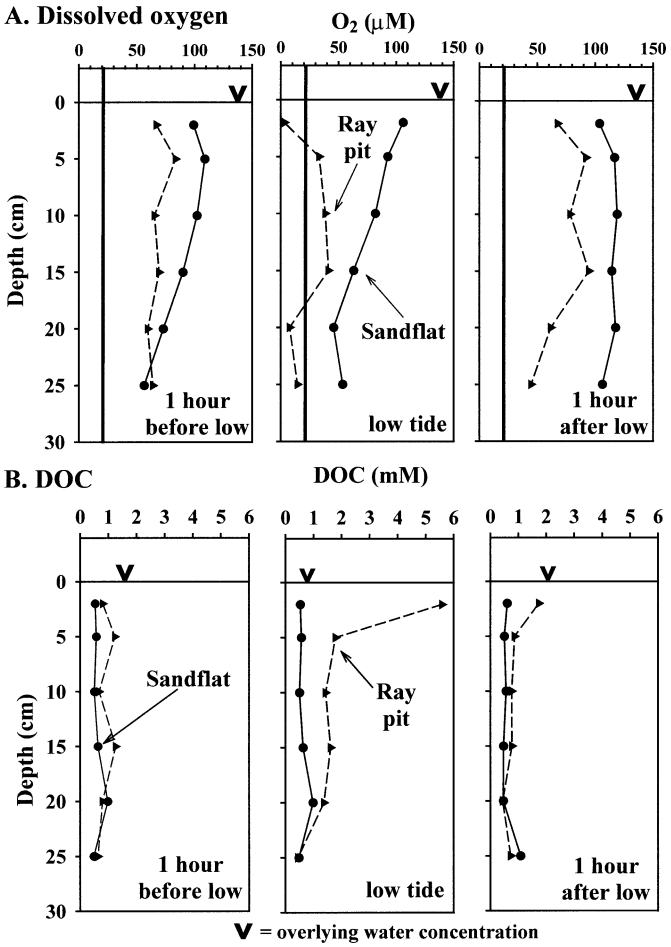

Fig. 7. Porewater profiles of (A) dissolved oxygen and (B) DOC for the sand flat and within a ray pit on 19 August 1998. The solid vertical bar in panel A represents the lower detection limit of dissolved oxygen when the microwinkler technique is used. Any sample equal to or less than this value was assumed to be anoxic.

irrigating shrimp maintained a relatively vertical ammonium profile. This was not maintained in the sandflat, which showed higher ammonium concentrations at all depths. After the onset of flood tide, ammonium was rapidly flushed out of the sandflat to a depth of 25 cm, reestablishing concentrations noted before low tide. Ammonium values associated with shrimp burrows were of similar magnitude to profiles measured at the other two time points. Figure 6B shows total nitrate and nitrite concentrations at the same depths and times as the ammonium figure. Profiles of NO_3-NO_2 for the sandflat were essentially vertical, with some depression at low tide. Concentrations were 50%–200% higher in the vicinity of active *C. major* burrows. This pattern was only evident at slack low tide, when porewater advection was minimized. These patterns were only observed on 20 August 1998; ammonium and nitrate-nitrite profiles in the vicinity of shrimp burrows were comparable to sandflat profiles on 18 August.

Solute profiles within ray pits—The presence of ray pits had a distinct impact on porewater nutrient profiles that apparently was related to reduced flushing in the vicinity of these structures. The concentration profiles of dissolved oxygen associated with ray pits were lower than the sandflat (Fig. 7A). In addition, there were low oxygen spikes associated with the accumulation of fine sediments in the ray pit (2 cm). There was a drop in dissolved oxygen in both sampled environments at low tide, with almost the entire ray pit profile going anoxic. In contrast, only the two deepest intervals in the sandflat are low in oxygen. After 1 h into the flood tide, the entire profile in the sandflat was reoxygenated to overlying water concentrations. Flushing of dissolved oxygen into the sediments beneath the ray pit was also evident, but the concentrations are much lower than those measured in the sandflat and overlying water.

Figure 7B shows the results for DOC profiles on the same porewater samples used for dissolved oxygen analyses (Fig. 7A). DOC concentrations showed elevated concentrations in ray pits. There was little change in sandflat DOC profiles, but ray pits showed a distinct ingrowth of DOC concentrations in the top 20 cm at low tide. The 2-cm depth interval at low tide showed the greatest effect of the ray pit, with DOC concentrations ~10 times the measured concentration

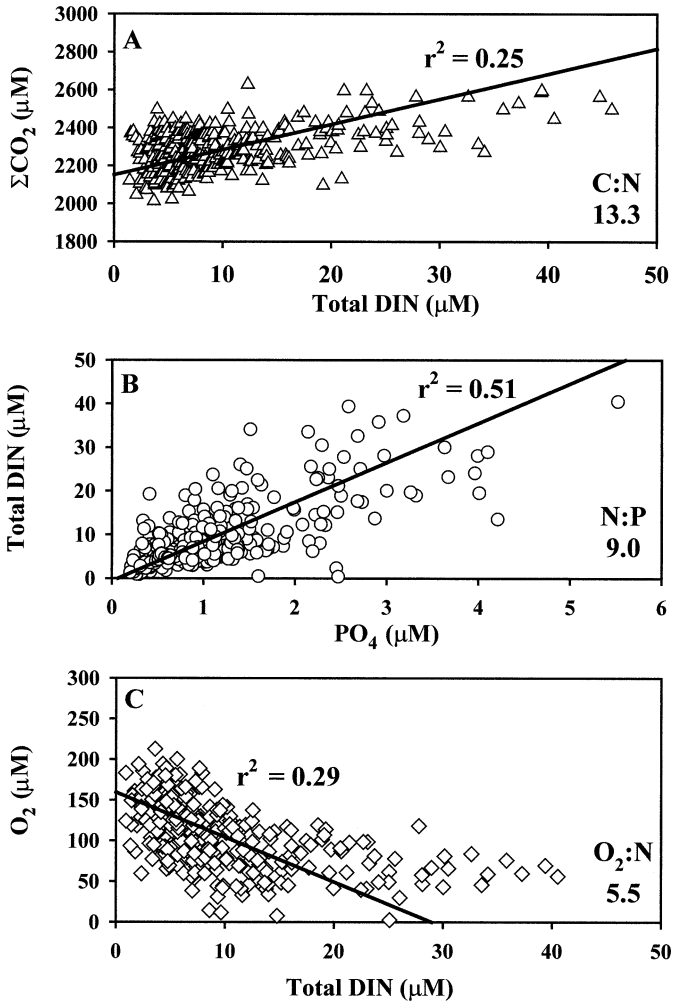

Fig. 8. Geometric mean regressions of the net stoichiometric relationships among (A) C : N, (B) N : P, and (C) O_2 : N for all 7 d that porewater sipper data were collected. The R^2 values for the regressions were 0.25, 0.51, and 0.29 for C : N, N : P, and O_2 : N, respectively.

in the sandflat. This general pattern was maintained 1 h into the flood tide, although the concentrations had decreased.

Porewater sippers stoichiometry—Figure 8 shows the apparent C : N, N : P, and O_2 : N stoichiometries from the porewater sipper samples. Because transport is dominated by advection, it is assumed that solute fractionation during transport is minimal. However, differential adsorption behavior may compromise this simple assumption. The C : N ratio is approximately twice the Redfield ratio (6.6), although most of the values are clustered at one end of the figure because of the low DIN and relatively constant ΣCO_2 values measured. Correction for nonsteady effects of NH_4^+ adsorption would lower the apparent ratio to ~8.1. This estimate is a maximum because of a lack of correction for denitrification. The N : P ratio for this system is ~9, ~60% of the prediction based on the Redfield ratio (~16). This ratio is also potentially affected by adsorption, P more so than N (e.g., Krom and Berner 1980), which implies that it is likely a maximum and reenforces conclusions of either P-rich substrate or differential loss of N (denitrification). The data indicate an O_2 : N ratio lower (N-rich) than the Redfield prediction (8.6). The deviation from the predicted regression at low dissolved oxygen concentrations occurs when ammonium dominates total DIN concentrations.

Discussion

Seasonal flux and fate of organic matter on Debidue Flat—Organic matter (OM) remineralization and tidally driven exchange in the permeable sands of Debidue Flat resulted in the dynamic, rapid release of products of early diagenesis into porewater and overlying water on timescales of hours and over depth scales of ≥30 cm. Our measurements showed that the magnitudes of reactive carbon fluxes through Debidue Flat were high, had a strong seasonal component, and were spatially heterogenous depending on the local interplay among physical and biological structure, activity, and water flow. Despite low organic C contents (~0.04%), the magnitude of the carbon remineralization fluxes measured on Debidue Flat (~20–170 mmol m^{-2} d^{-1}) were similar to those measured in other intertidal, salt marsh, subtidal, and deltaic sediments and orders of magnitude greater than carbon fluxes measured on the continental margin (Table 2).

The seasonal pattern and magnitude of reactive carbon fluxes in the sandflat were comparable to or greater than rates of sulfate reduction measured in adjacent surficial deposits within salt marsh areas of the North Inlet estuary (King 1988). Although fall and winter sandflat remineralization rates were similar to nearby salt marsh rates (Table 3), June 1998 incubations predicted fluxes up to five times

Table 2. Comparison of carbon fluxes from this study to measured ΣCO_2 fluxes from other coastal systems. Fluxes for North Inlet, Flax Pond, Westerschelde estuary, and Long Island Sound were based on values measured in the fall for direct comparison. S, converted from sulfate reduction rates.

Description	Location	J_c (mmol C m^{-2} d^{-1})	Reference
Intertidal sandflat	N. Inlet, SC	44–58	This study
Intertidal flats, saline end members	Westerschelde, Netherlands	~50–90	Middelburg et al. (1996)
Salt marsh	N. Inlet, SC	36–100 (S)	King (1988)
Salt marsh	Flax Pond, NY	25–160	Mackin and Swider (1989)
Deltaic sediments	Amazon Shelf	10–70	Aller et al. (1996)
Subtidal muddy	LIS, NY	17–33	Mackin and Swider (1989)
Continental slope/rise	Central CA	0.9–3.8	Reimers et al. (1992)

Table 3. Comparison of seasonal carbon fluxes on Debidue Shoal to North Inlet salt marsh carbon fluxes in the vicinity of *S. alterniflora* computed from sulfate reduction rates (after King 1988).

Dates (this study)	T (°C)	C flux (mmol m^{-2} d^{-1})	Dates (king 1988)	T (°C)	C flux (mmol m^{-2} d^{-1})
Fall 1997 (Sep)	28	44–58	Fall (Oct 1984)	~22	~36–100
Winter 1998 (Jan)	16	22–39	Winter (Jan 1985, Feb 1986)	~4–17	~10–40
Summer 1998 (Jun)	30	155–170	Summer (Jun 1986, Jul 1984)	~26	~30–110

ΣCO_2 fluxes estimated from sulfate reduction (King 1988). The June incubation corresponds to the beginning of the annual summer chlorophyll maximum in North Inlet (Lewitus et al. 1998), which may have had an impact on reactive carbon supply to the sandflat. This is reflected in Chl *a* profiles measured during this time period. Surface Chl *a* values (8 nmol g^{-1}) in June 1998 were double that measured at any other time point (Fig. 5).

The data on remineralization rates discussed above come from cores held under closed conditions. In permeable sandy systems, the rapid supply of oxidants and reactive substrates, and the rapid removal of end products likely control decomposition processes (e.g., Huettel and Webster 2001). Thus it is likely that the in situ reaction rates are higher than those measured in the core incubations where Debidue Flat sediments are forced into a diffusional transport regime. The closed system approach used in these experiments to measure remineralization does have some limitations but illustrate the relative patterns and magnitude of organic matter remineralization on Debidue Flat.

The measured OC fluxes quantify seasonal carbon supply for Debidue Flat but do not by themselves indicate the quality or nature of the OM driving decomposition. The penetration of high Chl *a* concentrations to depths of ~25 cm (Fig. 5), and concentrations above background to depths of 40 cm implicate algal debris as a labile carbon source for this system. A simple calculation was done to demonstrate the potential of algal-derived carbon as the primary source of reactive OC in this system. The surface Chl *a* concentration in surface sediments was 7.2 μg g^{-1} (Fig. 5). When an OC : Chl *a* ratio of ~60 was used, a quantity of algal-derived OC of ~430 μg g^{-1} or 0.04% dry weight resulted. This is comparable to the measured OC (0.04%) in the surface sediments of Debidue Flat and could account for all of the measured OC. Even if the lower values from fall 1997 and winter 1998 were used (2 and 4 nmol Chl *a* g^{-1}), algal derived carbon could account for 25%–100% of the measured OC in sandflat sediments.

Table 4. Comparison of estimates of ΣCO_2 flux during the seasonal incubations, measured microalgal production on intertidal sandflats (Pinckney and Zingmark 1993*a*,*b*) and gross primary production (Sellner et al. 1976) for North Inlet estuary.

Month	ΣCO_2 flux (mmol C m^{-2} d^{-1})	Microalgal production (Pinckney and Zingmark 1993*a*,*b*) (mmol C m^{-2} d^{-1})	Primary production (Sellner et al. 1976) (mmol C m^{-2} d^{-1})
Sep	44	27	260
Jan	22	23	16
Jun	155	35	230

The most likely sources of phytopigments to Debidue Flat were benthic microalgal production and benthic filtration of water column phytoplankton (Huettel and Rusch 2000). The presence of benthic microalgal communities throughout the year could provide a constant source of labile OC to Debidue Flat. Table 4 compares the lower estimates of ΣCO_2 flux during the seasonal incubations to measured benthic microalgal production on intertidal sandflats (Pinckney and Zingmark 1993*a*,*b*) and gross primary production (Sellner et al. 1976) for North Inlet estuary. Estimated reactive carbon fluxes indicated that 99%–100% of the microalgal production and 15%–59% of the total primary production (water column plus microalgal production) in the system could be remineralized in the sandflat sediments. The rapid remineralization of microalgal carbon clearly creates a feedback mechanism whereby inorganic nutrients released by decomposition are rapidly available to the surface microalgal community and stimulate its growth.

Advective flushing of sandy sediments due to overlying water currents has been shown to contribute viable algal particles to significant depths given high permeability (e.g., Huettel et al. 1996; Huettel and Rusch 2000). This is a potentially important mechanism for reactive carbon supply to Debidue Flat sediments. General likely limits on benthic filtration of overlying water phytoplankton can be evaluated by use of Chl *a*. For example, under the assumption of the June 1998 sediment inventory of Chl *a* (top 5 cm, 31.9 nmol cm^{-2}, Fig. 5) and an average decomposition rate coefficient of ~ 0.13 d^{-1} (30°C, Sun et al. 1993), then the flux of Chl *a* required to support the sediment inventory at steady state is ~4.1 nmol cm^{-2} d^{-1}. Given an average overlying water Chl *a* concentration of ~13.4 nmol L^{-1} (10-yr June average, Lewitus et al. 1998), then ~310 cm^3 cm^{-2} d^{-1} of overlying water would have to be filtered through the upper sandflat surface to produce the entire Chl *a* inventory (100% efficient extraction). This flow rate would correspond to a porewater turnover time of ~9 min (which assumes a porosity of 0.4, 2 cm^3 porewater). In contrast, if a pore water turnover rate of ~ 2 d is used (derived from ΣCO_2 production Table 5), then ~0.3% of the sedimentary Chl *a* pool could be accounted for by water column filtration. These calculations clearly demonstrate that contributions of benthic and pelagic production to sedimentary remineralization could vary widely depending on local conditions. They show that there are multiple ways of supplying substrate, all of which are capable of accounting for the observed magnitudes within reasonable uncertainties. If we accept factors of two uncertainty

Table 5. Summary of values used for porewater exchange time calculations. Data used included the initial measured ΣCO_2 and NH_4^+ profiles, $C(z)$, and the production rate, $R(z)$, estimated from the winter and summer 1998 whole-core incubations. Porewater exchange time (t) can be calculated by the relationship: $\tau = (C[z])/(R[z])$ where t is the exchange time in days; $C(z)$ is the initial concentration at depth z (mM ΣCO_2 or μM NH_4^+), and $R(z)$ is the reaction rate at depth z estimated from the incubations (mM ΣCO_2 d^{-1} or μM NH_4^+ d^{-1}). The data used represent the two possible extremes for porewater exchange time in these experiments.

z (cm)	Winter $C(z)$ (mM C)	Winter $R_C(z)$ (mM d^{-1})	Winter τ (d)	Winter $C(z)$ (μM N)	Winter $R_N(z)$ (μM d^{-1})	Winter τ (d)	Summer $C(z)$ (mM C)	Summer $R_C(z)$ (mM d^{-1})	Summer τ (d)	Summer $C(z)$ (μM N)	Summer $R_N(z)$ (μM d^{-1})	Summer τ (d)
2.5	2.6	0.27	10	3.3	39.8	0.1	3.3	1.4	2	7.3	73.6	0.1
7.5	2.9	0.18	16	16.16	32.6	0.5	3.2	0.80	4	16.4	59.9	0.3
12.5	2.8	0.13	22	43.6	21.4	2	3.1	0.79	4	26.2	43.1	0.6
17.5	2.6	0.11	24	50.4	16.9	3	3.0	0.78	4	20.9	31.8	0.7
25	2.2	0.10	22	22.2	6.7	3	2.9	0.78	4	20.7	14.0	1.5
35	2.1	0.09	23	11.9	8.5	1	3.0	0.78	4	13.5	11.9	1.1

in any of several parameters, one can readily bracket observations.

Model calculations of decomposition rates are consistent with an algal source as a primary component of the reactive carbon pool. The estimated first-order reactivities (k = 0.022 d^{-1}, 0.023 d^{-1}) and corresponding half-lives ($t_{1/2}$ = 31.5 d, 30 d) (Fig. 4) are similar to values calculated for sedimented phytoplankton (Middelburg 1989; Sun et al. 1991) and macrophyte detritus (Bianchi and Findlay 1991). These results, combined with evidence from seasonal Chl *a* profiles and inventories, imply that OC remineralization processes on Debidue Flat are dominated by a labile OC source, most likely algal in origin, that is rapidly mineralized.

In a case where labile algal cells are the sole source of OC, we would expect low net C : N stoichiometry at depths where Chl *a* is measured. In both the winter and summer incubations, Chl *a* concentrations showed little change from the 15–30 cm depth (Fig. 5). In contrast, the net C : N stoichiometry of decomposition in the sandflat cores increased 2–3 times over these same depths (Fig. 2). The rapid attenuation of NH_4^+ production rates relative to ΣCO_2 in the whole-core incubations (Fig. 1) and resultant steady increase in C : N ratio with depth implied either a more refractory substrate at depth and/or immobilization of nitrogen into microbial biomass. In contrast, the presence of *C. major* burrows stabilizes the net C : N ratio of decomposition with depth (discussed in more detail in the Macrobiological Impacts section below).

During microbial decomposition of OM, part of the organic nitrogen decomposed is converted to microbial biomass and part is remineralized to inorganic nitrogen (e.g., Broadbent and Nakashima 1970; Mundra et al. 1973; Janssen 1996). If an organic substrate is low in nitrogen, microbes can take up inorganic nitrogen from solution, resulting in a lower net release of inorganic nitrogen during remineralization than is stoichiometrically present in the degraded sources. The most common refractory OM in North Inlet is *Spartina alterniflora* detritus. This material has a high C : N ratio (90–100), and its decomposition is characterized by a net decrease in OC and a rapid increase in organic nitrogen associated with microbial biomass (e.g., Odum and de la Cruz 1967; Benner et al. 1991; White and Howes 1994). Growth of bacteria on *Spartina* detritus in the sediments of Debidue Flat could provide a sink for inorganic nitrogen released during the rapid remineralization of marine algal material. This uptake would result in lower net inorganic nitrogen production in the incubations and could account for the high net C : N ratios at depth in these experiments where algal sources are depleted and more refractory substrates dominate. On the basis of the C : N ratios of algae (7, Hillebrand and Sommer 1999) and *Spartina* detritus (~100), 20%–85% of the total OC remineralized at depth (>30 cm) would have to be *Spartina* detritus to produce the maximum measured net C : N ratios (25–90).

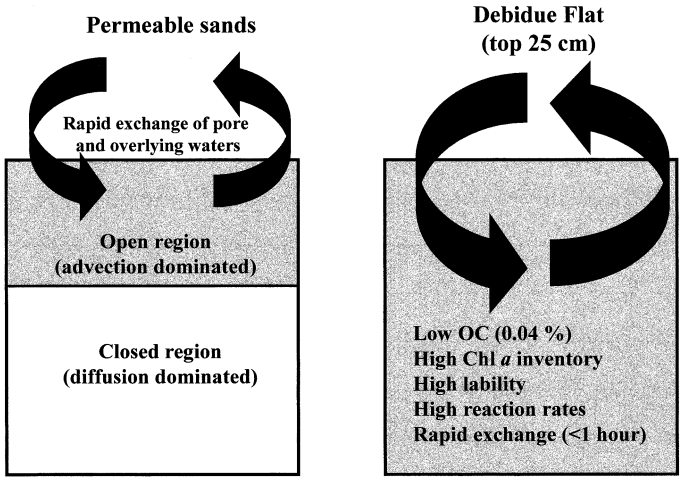

Fig. 9. Conceptual figure of the open and closed regions of permeable sandy sediments and the characteristics of the open region of the permeable sands in Debidue Flat.

Permeable sandflats as dynamic open systems—OM decomposition in permeable sands is influenced by the rapid exchange of pore and overlying waters produced by advective flow within an ''open'' region and an underlying ''closed'' diffusion-dominated region (Fig. 9). The factors that primarily control the depth and importance of this open region include particulate organic carbon (POC) supply, sediment permeability, bottom currents, and OM lability (see Huettel et al. 1998; Huettel and Rusch 2000; Huettel and Webster 2001). The significance of the open region in permeable sands is that these regions are thought to be efficient

particulate organic matter filters and to accelerate OM remineralization and nutrient cycling (Huettel and Rusch 2000).

The closest engineering parallel to these functions are municipal slow sand filters. These filters typically consist of a 0.5–1.2 m filter bed of fine sand through which water percolates, which results in a decrease of OM and turbidity by a combination of biological (microbial degradation and algal assimilation) and physical (filter skin or *schmutzdecke* and adsorption) processes (Huisman and Wood 1974; Visscher 1990). The major drawback to slow sand filters is clogging during high turbidity. In a municipal filter, clogging is corrected by scraping off the filter skin and restarting the filter. In marine systems, the efficiency of permeable sands as biofilters will depend on physical (physical mixing and resuspension of sediments) and biological (e.g., bioturbation) processes that prevent or minimize clogging. There must be a close coupling between permeability, which allows rapid flux and turnover, and mineralization, which removes OC.

The rapidly exchanged ''open'' region in Debidue Flat extends to a depth of at least 25 cm and is characterized by low POC content, high Chl *a* inventories, high OM lability and remineralization rates, and low porewater nutrient concentrations. Tidally driven porewater advection and biogenic irrigation maintain essentially vertical profiles of reactive porewater constituents despite high reaction rates. Rough estimates of porewater turnover time can be made by simply dividing the average porewater concentrations by production rates (Fig. 1). In the case of NH_4^+, calculated turnover times of ~0.1–0.5d result and are presumably dominated by transport-driven exchange. The maintenance of the surficial open region on Debidue Flat requires high permeability and high tidal current speeds. High permeability on Debidue Flat is maintained by a combination of sediment supply, physical mixing, high mineralization rates, and bioturbation to at least 30 cm. Humphries (1977) demonstrated that sediment erosion and deposition on Debidue Flat exchanges well-sorted medium-fine sand between the sand flat and nearby beaches. Near-bed tidal current velocities on Debidue Flat are typically 27–33 cm s^{-1} (Grant 1981), but tidal velocities in the portion of North Inlet over Debidue Flat have been measured up to 90 cm s^{-1} (Kjerfve and Proehl 1979). These high velocities effectively mix the top 2–5 cm of the sandflat during ripple migration (Grant 1983; D'Andrea et al. unpubl. data), maintaining the high permeability in the surface sediments. The top 30 cm of Debidue Flat are inhabited by haustoriid amphipods (*Acanthohaustorius millsi* and *Pseudohaustorius caroliniensis*) in densities of 10^5 m^{-2}, which have been implicated in the high biodiffusive mixing measured on the sandflat (D'Andrea et al. unpubl. data). Thus, bioturbation by these amphipods may also play an important role in maintaining the high permeability to 25 cm necessary for the open region to persist.

The role of porewater advection in flushing the sediments of Debidue Flat can be evaluated by comparing changes in porewater solutes on the basis of independent measures of reaction rates in this system. Table 5 shows the porewater exchange time on Debidue Flat based on measured winter and summer reaction rates. These exchange times range from 0.1 to 24 d, depending on season and whether C or N residence time calculations are used. The porewater sipper experiments demonstrated that the exchange times for the top 25 cm of Debidue Flat are actually on the order of 1–2 h (Figs. 6, 7). These results indicated that advective porewater flow is primarily responsible for the porewater solute profiles measured on Debidue Flat, and only at slack low tide can in situ remineralization processes be separated from the dominant advective effects.

Analyzing the stoichiometry of changes in oxygen, carbon, nitrogen, and phosphorus provides information on the nature of the substrate undergoing decomposition, which can be compared to Redfield ratios (Redfield 1958). The r^2 values are generally low (0.25–0.5) but show the general relationships between the carbon, nitrogen, and phosphate components of Debidue Flat (Fig. 8). The O_2 : N and N : P ratios indicate that a nitrogen-rich substrate, probably algal in origin, is undergoing decomposition on Debidue Flat. The N : P ratio is ~60% of the prediction based on Redfield ratios, which implies high denitrification rates. The actual ratio is even lower because the phosphate values have not been corrected for adsorption. Although there is substantial uncertainty, the net stoichiometries indicated that a relatively nitrogen and phosphate rich substrate undergoing denitrification was being remineralized in this system. These properties are indicative of the early stages of decomposition of a fresh, reactive substrate, in this case most likely algal in origin. These results support a ''biofilter'' analogy for intertidal sandflats, where dissolved and particulate OM is rapidly supplied and remineralized with the products rapidly flushed out of the system (Huettel and Rusch 2000).

Macrobiological impacts on OM flux and remineralization—The depth attenuations of carbon and ammonium reaction rates were directly impacted by the presence of *C. major* burrows. Carbon reaction rates associated with shrimp burrows were greater at all depths relative to sandflat cores in the fall and winter incubations. Ammonium reaction rates in the vicinity of *C. major* burrows showed the greatest departure from depth-dependent patterns predicted from surrounding sandflat sediments. At depths of 10–15 cm, the reaction rates associated with shrimp burrows leveled off. The ammonium production rates at 40 cm near *C. major* burrow walls were comparable to reaction rates at 10–15 cm in the surrounding sandflat. These patterns result in a relatively constant C : N ratio of decomposition rather than the consistent increase with depth noted in the sandflat cores (Fig. 2).

The greatest impact of shrimp burrows can be seen at depths >15 cm and is consistent with *C. major* burrow structure. The vertical portion of their burrows consist of three sections: a narrow (5–8 mm diameter) shaft 5–20 cm long, a middle section 10–15 cm long gradually widening, and the main portion of the burrow, which has a uniform diameter depending on animal size (1.5–2.5 cm diameter) (Pohl 1946; Weimer and Hoyt 1964; Frey et al. 1978). The middle and main sections of the burrow are the more permanent portions of the burrow and are lined with sandy mud bound with gelatinous mucus in the form of round pellets (Frey et al. 1978). Burrow linings of other callianassid shrimps have 4.5–15 times more OC than ambient sediments

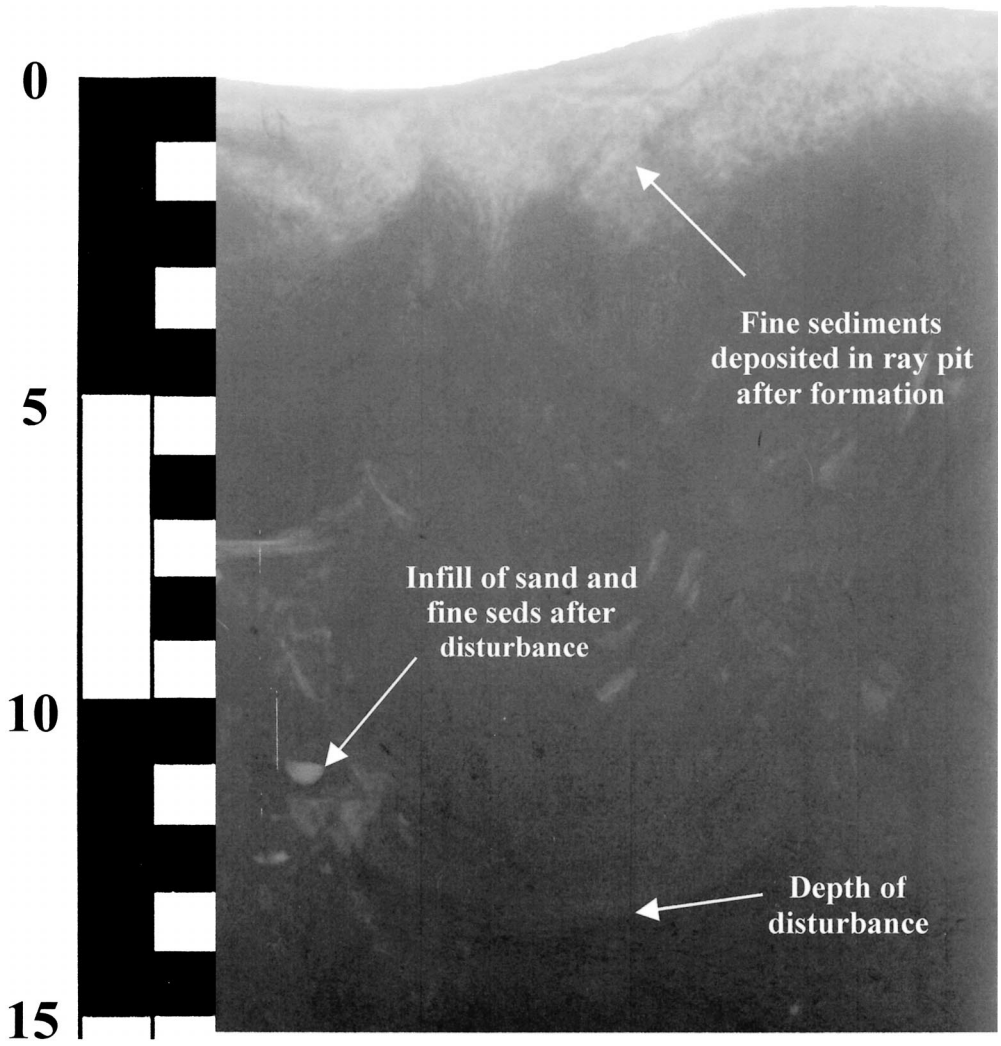

Fig. 10. Positive scanned image of an x-ray of a ray pit structure. The scale on the left side of the image is in centimeters. Note the fine sediments collected within the ray pit after formation, the depth of the disturbance (here ~15 cm), and the infill of sand and fine sediments along the edges of the disturbance.

and are the focal points of subsurface biomass of aerobic and anaerobic microbes (Dobbs and Guckert 1988; De Vaugelas and Buscail 1990). Burrow walls are a geochemically important sink for OC and play an important role in reaction rates and fluxes at depth in the sandflat.

The main impact of irrigation and feeding activity of *C. major* was seen at low tide, when lack of physical forcing allows the isolation of biogenic irrigation from impressed advection. At slack low tide but with water still over the burrows, the actively burrowing shrimp maintain a relatively vertical ammonium profile in the sediments. The NH_4^+ concentrations associated with *C. major* burrows were higher than those measured in the sandflat, particularly at depths >15 cm where ammonium production rates are two–four times greater than the sand flat (Fig. 1). The higher reaction rates associated with *C. major* burrows and the ingrowth of ammonium profiles associated within the ambient sandflat indicated an increased flux of ammonium out of shrimp burrows or local consumption during reaction. There was also high nitrification associated with *C. major* burrows that was only evident at low tide when porewater advection was minimized.

These porewater inorganic nitrogen patterns were only observed on one of the two days that sipper data was collected around *C. major* burrows but were consistent with studies that have investigated nutrient fluxes associated with irrigating infauna. Benthic communities increase the NH_4^+ flux out of sediments (Henrikson et al. 1980, Ziebis et al. 1996*b*) and enhance the rates of nitrification and denitrification (see reviews by Aller 1988, 2001; Kristensen 1988). Burrows, in particular, can play an important role in regulating the inorganic nitrogen flux at the sediment-water interface. Ammonium fluxes across burrow walls at depth in the sediment are similar in magnitude to nearshore surface sediment fluxes (e.g., Aller and Yingst 1978; Kristensen 1984), effectively increasing the surface area across which inorganic nitrogen can be exchanged with the overlying water. The increased flux of ammonium and increased nitrification and denitrifi-

cation inferred for *C. major* burrows based on the porewater profiles in these experiments imply that burrowing shrimp play an important role in nitrogen cycling on Debidue Flat.

Porewater solute patterns in the vicinity of ray pits showed evidence for rapid remineralization of organic matter in the sediments below these structures and slowed flushing in the vicinity of these structures. Ray pits are large (30–80 cm diameter) biogenic disturbances that occurred from April through November on Debidue Flat, covered ~1–3% of the surface area of the sand flat, and persisted for 1–4 days (D'Andrea et al. unpubl. data). They alter the structure of sediments to at least 15 cm (Fig. 10). Thus, these structures can be considered localized, seasonal, short-term depositional centers for reactive OM. The initial infilling of the disturbance results in the burial of both sand and fine sediments. During the short residence time (1–4 days) of these structures, fine sediments settle out of the water into the pit. The aspect ratio (depth to diameter) associated with these features can permit separation of overlying flow from flow within the pits, resulting in increased particulate flux to the base of the pit (Yager et al. 1993). Their role in the localized supply of reactive OM is particularly important in sands where high current speed typically prevent settlement of finer sediments.

The rapid loss of dissolved oxygen and production of DOC in the porewaters beneath the ray pit relative to the sandflat can be explained by either increased remineralization rates associated with these structures and/or an increase in reactive carbon supply. The ΣCO_2 reaction rates within ray pits were generally lower or comparable to those measured for the sandflat (unpubl. data) and implicate the mass input of reactive carbon in ray pits for the rapid response of solute profiles in the absence of porewater advection. These results are consistent with the increased flux of fine particles and associated OM predicted for ray pits (Yager et al. 1993) and the high *C. major* fecal pellet densities measured within ray pits on Debidue Flat (D'Andrea unpubl. data).

In addition to supplying reactive OM, the presence of ray pits decreased the impact of tidally driven advective porewater flux. In contrast to solute patterns associated with the sand flat and *C. major* burrows, solutes building up in the porewaters beneath ray pits were not rapidly flushed out of the sediment. This implied that the fine particles within ray pits limited the ability of tidally driven porewater advection to flush products of decomposition out of the sediment. The increase in fine particles would locally decrease the permeability of the surface sediments of the sandflat. Interstitial solute transport is strongly dependent on sediment permeability (Huettel and Gust 1992; Forster et al. 1996; Ziebis et al. 1996*a*), so the magnitude of advective solute transport should be less beneath ray pits relative to the rest of the sandflat.

This ''clogging'' mechanism observed on Debidue Flat on short temporal scales (<4 d) may be more significant both in scale and duration in other permeable sand environments. For example, if a permeable shelf system is dominated by physical mixing during a portion of the year (e.g., winter storms) followed by periods of overlying water productivity and decreased physical forcing, it is not unreasonable to hypothesize that the efficiency and depth of the ''open'' region could decrease over this period. Quantifying the dynamics of changing permeability and subsequent changes in carbon cycling through permeable sediments is an important step in understanding the role of permeable sediments in global carbon biogeochemical cycles.

Despite low OC concentrations (~0.04%), the magnitudes of reactive carbon fluxes through Debidue Flat were high (44–170 mmol C m^{-2} d^{-1}), had a strong seasonal component, and were comparable to fluxes measured in many organic-rich deposits. The substrate being remineralized on Debidue Flat has a high reactivity (first-order rate constant: $k \sim 0.02$ d^{-1}), is primarily oxidized to ΣCO_2 (~90%; ~10% to DOC), and an N-, P-rich character (N : P ~ 9). These results, combined with the deep penetration of Chl *a*, imply a marine algal or bacterial source for OM in this system.

Porewater solute profiles were controlled by advective flow that rapidly exchanged porewaters over ~30 cm on an hourly or daily basis. The dynamic porewater reservoir in Debidue Flat is the result of a close coupling between permeability, permitting rapid flux and turnover, and mineralization, which removes OC. This coupling permits the sandflat to act like an unsteady ''trickling bed filter'' efficiently burning off organic material and resulting in low residual OC (~0.04% by weight sediment) despite high year-round fluxes. As illustrated by Debidue Flat, intertidal sands can be sites of high OM flux and turnover and play an important role in biogeochemical cycling in estuarine systems.

References

ALLER, R. C. 1988. Benthic fauna and biogeochemical processes in marine sediments: The role of burrow structures, p. 301–338. *In* T. H. Blackburn and J. Sorensen [eds.], Nitrogen cycling in coastal marine environments. Wiley.

———. 2001. Transport and reactions in the bioirrigated zone, p. 269–301. *In* B. P. Boudreau and B. B. Jorgensen [eds.], The benthic boundary layer. Oxford Univ. Press.

———, N. E. BLAIR, Q. XIA, AND P. D. RUDE. 1996. Remineralization rates, recycling, and storage of carbon in Amazon shelf sediments. Cont. Shelf Res. **16:** 753–786.

———, AND J. MACKIN. 1989. Open-incubation, diffusion methods for measuring solute reaction rates in sediments. J. Mar. Res. **47:** 411–440.

———, AND J. YINGST. 1978. Biogeochemistry of tube dwellings: A study of the sedentary polychaete *Amphitrite ornata* (Leidy). J. Mar. Res. **36:** 201–254.

BENNER, R., M. L. FOGEL, AND E. K. SPRAGUE. 1991. Diagenesis of belowground biomass of *Spartina alterniflora* in salt-marsh sediments. Limnol. Oceanogr. **36:** 1358–1374.

BIANCHI, T. S., AND S. FINDLAY. 1991. Decomposition of Hudson River macrophytes: Photosynthetic pigment transformations and decay constants. Estuaries **14:** 65–73.

BROADBENT, F. E., AND T. NAKASHIMA. 1970. Nitrogen immobilization in flooded soils. Soil Sci. Soc. Am. Proc. **34:** 218–221

CAMMEN, L. 1991. Annual bacterial production in relation to benthic microalgal production and sediment oxygen uptake in an intertidal sandflat and an intertidal mudflat. Mar. Ecol. Prog. Ser. **71:** 13–25.

DE VAUGELAS, J., AND R. BUSCAIL. 1990. Organic matter distribution in burrows of the thalassinid crustacean *Callichirus laurae*, Gulf of Aqaba (Red Sea). Hydrobiologia **207:** 269–277.

DOBBS, F. C., AND J. B. GUCKERT. 1988. *Callianassa trilobata* (Crustacea: Thalassinidae) influences abundance of meiofauna

and biomass, composition, and physiological state of microbial communities within its burrow. Mar. Ecol. Prog. Ser. **45:** 69–79.

FORSTER, S., M. HUETTEL, AND W. ZIEBIS. 1996. Impact of boundary layer flow velocity on oxygen utilization in coastal sediments. Mar. Ecol. Prog. Ser. **143:** 173–185.

FREY, R. W., J. D. HOWARD, AND W. A. PRYOR. 1978. *Ophiomorpha:* Its morphologic, taxonomic, and environmental significance. Paleogeogr. Paleoclimatol. Paleoecol. **23:** 199–229.

GRANT, J. 1981. Sediment transport and disturbance on an intertidal sandflat: Infaunal distribution and recolonization. Mar. Ecol. Prog. Ser. **6:** 249–255.

———. 1983. The relative magnitude of biological and physical sediment reworking in an intertidal community. J. Mar. Res. **41:** 673–689.

———, C. W. EMERSON, B. T. HARGRAVE, AND J. L. SHORTLE. 1991. Benthic oxygen consumption on continental shelves off Eastern Canada. Cont. Shelf Res. **11:** 1083–1097.

HENRIKSON, K., J. HANSEN, AND T. BLACKBURN. 1980. The influence of benthic infauna on exchange rates of inorganic nitrogen between sediment and water. Ophelia Suppl. **1:** 249–256.

HILLEBRAND, H., AND U. SOMMER. 1999. The nutrient stoichiometry of benthic microalgal growth: Redfield proportions are optimal. Limnol. Oceanogr. **44:** 440–446.

HUETTEL, M. 1990. Influence of the lugworm *Arenicola marina* on porewater nutrient profiles of sand flat sediments. Mar. Ecol. Prog. Ser. **62:** 241–248.

———, AND G. GUST. 1992. Solute release mechanisms from confined sediment cores in stirred benthic chambers and flume flows. Mar. Ecol. Prog. Ser. **82:** 187–197.

———, AND A. RUSCH. 2000. Transport and degradation of phytoplankton in permeable sediment. Limnol. Oceanogr. **45:** 534–549.

———, AND I. T. WEBSTER. 2001. Porewater flow in permeable sediments, p. 144–179. *In* B. P. Boudreau and B. B. Jorgensen [eds.], The benthic boundary layer. Oxford Univ. Press.

———, W. ZIEBIS, AND S. FORSTER. 1996. Flow-induced uptake of particulate matter in permeable sediments. Limnol. Oceanogr. **41:** 309–322.

———, ———, ———, AND G. W. LUTHER III. 1998. Advective transport affecting metal and nutrient distributions and interfacial fluxes in permeable sediments. Geochim. Cosmochim. Acta **62:** 613–631.

HUISMAN, L., AND W. E. WOOD. 1974. Slow sand filtration. World Health Organization.

HUMPHRIES, S. M. 1977. Seasonal variation in morphology at North Inlet, SC. M.S. thesis, Univ. of South Carolina, Columbia.

JANSSEN, B. H. 1996. Nitrogen mineralization in relation to C : N ratio and decomposability of organic materials. Plant Soil **181:** 39–45.

KING, G. M. 1988. Patterns of sulfate reduction and the sulfur cycle in a South Carolina salt marsh. Limnol. Oceanogr. **33:** 376–390.

KJERVE, B., AND J. A. PROEHL. 1979. Velocity variability in a cross section of a well-mixed estuary. J. Mar. Res. **37:** 409–418.

KRISTENSEN, E. 1984. Effect of natural concentrations on nutrient exchange between a polychaete burrow in estuarine sediment and the overlying water. J. Exp. Mar. Biol. Ecol. **75:** 171–190.

———. 1988. Benthic fauna and biogeochemical processes in marine sediments: Microbial activities and fluxes, p. 275–299. *In* T. H. Blackburn and J. Sorensen [eds.], Nitrogen cycling in coastal marine environments. Wiley.

KROM, M. D., AND R. A. BERNER. 1980. The experimental determination of the diffusion coefficients of sulfate, ammonium, and phosphate in anoxic marine sediments. Limnol. Oceanogr. **25:** 327–337.

LEWITUS, A. J., E. T. KOEPFLER, AND J. T. MORRIS. 1998. Seasonal variation in the regulation of phytoplankton by nitrogen and grazing in a salt-marsh estuary. Limnol. Oceanogr. **43:** 636–646.

MACKIN, J. E., AND K. T. SWIDER. 1989. Organic matter decomposition pathways and oxygen consumption in coastal marine sediments. J. Mar. Res. **47:** 681–716.

MCLACHLAN, A. 1989. Water filtration by dissipative beaches. Limnol. Oceanogr. **34:** 774–780.

———, I. G. ELIOT, AND J. DES CLARKE. 1985. Water filtration through reflective microtidal beaches and shallow sublittoral sands and its implications for an inshore ecosystem in Western Australia. Estuar. Coast. Shelf Sci. **21:** 91–104.

MIDDELBURG, J. J. 1989. A simple rate model for organic matter decomposition in marine sediments. Geochim. Cosmochim. Acta **53:** 1577–1588.

———, G. KLAVER, J. NIEUWENHUIZE, A. WIELEMAKER, W. DE HAAS, T. VLUG, AND J.F.W.A. VAN DER NAT. 1996. Organic matter mineralization in intertidal sediments along an estuarine gradient. Mar. Ecol. Prog. Ser. **132:** 157–168.

MUNDRA, M. C., G. S. BHANDARIAND, AND O. P. SRISTAVA. 1973. Studies on mineralization and immobilization of nitrogen in soil. Geoderma **9:** 27–33.

ODUM, E. P., AND A. A. DE LA CRUZ. 1967. Particulate organic detritus in a Georgia salt marsh-estuarine system, p. 383–388. *In* G. H. Lauff [ed.], Estuaries. American Association for the Advancement of Science.

PINCKNEY, J. L., AND R. G. ZINGMARK. 1993*a*. Modeling the annual production of intertidal benthic microalgae in estuarine ecosystems. J. Phycol. **29:** 396–407.

———. AND ———. 1993*b*. Biomass and production of benthic microalgal communities in estuarine habitats. Estuaries **16:** 887–897.

POHL, M. E. 1946. Ecological observations on *Callianassa major* Say at Beaufort, North Carolina. Ecology **27:** 71–80.

REDFIELD, A. C. 1958. The biological control of chemical factors in the environment. Am. Sci. **46:** 205–222.

REIMERS, C. E., R. A. JAHNKE, AND D. C. MCCORKLE. 1992. Carbon fluxes and burial rates over the continental slope and rise off central California with implications for the global carbon cycle. Global Biogeochem. Cycles **6:** 199–224.

ROCHA, C. 1998. Rhythmic ammonium regeneration and flushing in intertidal sediments of the Sado estuary. Limnol. Oceanogr. **43:** 823–831.

———. 2000. Density-driven convection during flooding of warm, permeable intertidal sediments: The ecological importance of the convective turnover pump. J. Sea Res. **43:** 1–14.

ROSENFELD, J. K. 1979. Ammonium adsorption in nearshore anoxic sediments. Limnol. Oceanogr. **24:** 356–364.

ROWE, G. T., AND OTHERS. 1988. Benthic carbon budgets for the continental shelf south of New England. Cont. Shelf Res. **8:** 511–527.

SELLNER, K. G., R. G. ZINGMARK, AND T. G. MILLER. 1976. Interpretations of the ^{14}C method of measuring the total annual production of phytoplankton in a South Carolina estuary. Bot. Mar. **19:** 119–125.

SHUM, K. T., AND B. SUNDBY. 1996. Organic matter processing in continental shelf sediments—the subtidal pump revisited. Mar. Chem. **53:** 81–87.

SOLORZANO, L. 1969. Determination of ammonia in natural waters by the phenolhypochlorite method. Limnol. Oceanogr. **14:** 799–801.

STRICKLAND, J. D., AND T. R. PARSONS. 1972. A practical handbook of sea-water analysis. Fisheries Research Board of Canada.

SUN, M.-Y., R. C. ALLER, AND C. LEE. 1991. Early diagenesis of

chlorophyll-a in Long Island Sound sediments: A measure of carbon flux and particle reworking. J. Mar. Res. **49:** 379–401.

———, C. LEE, AND R. C. ALLER. 1993, Laboratory studies of oxic and anoxic degradation of chlorophyll-a in Long Island Sound sediments. Geochim. Cosmochim. Acta **57:** 147–157.

VANDERBORGHT, J.-P., R. WOLLAST, AND G. BILLEN. 1977. Kinetic models of diagenesis in disturbed sediments. Part 2. Nitrogen diagenesis. Limnol. Oceanogr. **22:** 794–803.

VISSCHER, J. T. 1990. Slow sand filtration: Design, operation, and maintenance. J. Am. Water Works Assoc. **82:** 67–71.

WEIMER, R. J., AND J. H. HOYT. 1964. Burrows of *Callianassa major* Say, geologic indicators of littoral and shallow neritic environments. J. Paleontol. **38:** 761–767.

WHITE, D. S., AND B. L. HOWES. 1994. Nitrogen incorporation into decomposing litter of *Spartina alterniflora*. Limnol. Oceanogr. **39:** 133–140.

YAGER, P. L., A. R. M. NOWELL, AND P. A. JUMARS. 1993. Enhanced deposition to pits: A local food source for benthos. J. Mar. Res. **51:** 209–236.

ZIEBIS, W., M. HUETTEL, AND S. FORSTER. 1996*a.* Impact of biogenic sediment topography on oxygen fluxes in permeable seabeds. Mar. Ecol. Prog. Ser. **140:** 227–237.

———, ———, AND B. B. JORGENSEN. 1996*b.* Complex burrows of the mud shrimp *Callianassa truncata* and their geochemical impact on the seabed. Nature **382:** 619–622.

Received: 29 June 2001
Accepted: 5 March 2002
Amended: 2 April 2002